Available online at www.sciencedirect.com
SCIENCE DIRECT®
Journal of Magnetic Resonance 162 (2003) 311–319
JMR Journal of Magnetic Resonance
www.elsevier.com/locate/jmr

Optimal control of spin dynamics in the presence of relaxation

Navin Khaneja,[a,*] Timo Reiss,[b] Burkhard Luy,[b] and Steffen J. Glaser[b]

[a] *Division of Applied Sciences, Harvard University, Cambridge, MA 02138, USA*
[b] *Institute of Organic Chemistry and Biochemistry II, Technische Universität München, 85747 Garching, Germany*

Received 7 October 2001; revised 4 December 2002

Abstract

Experiments in coherent spectroscopy correspond to control of quantum mechanical ensembles guiding them from initial to final target states. The control inputs (pulse sequences) that accomplish these transformations should be designed to minimize the effects of relaxation and to optimize the sensitivity of the experiments. For example in nuclear magnetic resonance (NMR) spectroscopy, a question of fundamental importance is what is the maximum efficiency of coherence or polarization transfer between two spins in the presence of relaxation. Furthermore, what is the optimal pulse sequence which achieves this efficiency? In this paper, we give analytical answers to the above questions. Unexpected gains in sensitivity are reported for one of the most commonly used experimental building blocks in NMR spectroscopy. Surprisingly, in the case when longitudinal relaxation is small, the relaxation optimized pulse elements (ROPE) that transfer maximum polarization between coupled spins are longer than conventional sequences.

1. Introduction

The control of quantum ensembles has many applications, ranging from coherent spectroscopy to quantum information processing. In most applications involving control and manipulation of quantum phenomena, the system of interest is not isolated but interacts with its environment. This leads to the phenomenon of relaxation, which in practice results in signal loss and ultimately limits the range of applications. Manipulating quantum systems in a manner that minimizes relaxation losses poses a fundamental challenge of utmost practical importance. A premier example is the control of coupled spin dynamics in nuclear magnetic resonance (NMR) spectroscopy [1]. In multidimensional NMR experiments, transfer of coherence between coupled nuclear spins is a crucial step. However with increasing size of molecules or molecular complexes, the rotational tumbling of the molecules becomes slower and leads to increased relaxation losses. When these relaxation rates become comparable to the spin–spin couplings, the efficiency of coherence transfer is considerably reduced, leading to poor sensitivity and significantly increased measurement times.

With recent theoretical advances, it has become possible to determine upper bounds for the efficiency of arbitrary coherence transfer steps in the absence of relaxation [2]. However, from a spectroscopist's perspective, some of the most important practical (and theoretical) problems have so far been unsolved:

(A) What is the theoretical upper limit for the coherence transfer efficiency in the presence of relaxation?
(B) How can this theoretical limit be reached experimentally?

The above raised questions can be addressed by methods of optimal control theory. The framework of optimal control theory was developed to solve problems like finding the best way to steer a rocket such that it reaches the moon, e.g., in minimum time or with minimum fuel. Here we are interested in computing the optimal way to steer a quantum system from some initial state to a desired final state with minimum relaxation losses. In this paper we introduce a class of control systems which gives analytical solutions to the above raised questions. It is shown that widely used standard NMR techniques are far from being optimal and surprising new transfer schemes emerge.

* Corresponding author. Fax: 1-617-496-6404.
E-mail address: navin@hrl.harvard.edu (N. Khaneja).

1090-7807/03/$ - see front matter © 2003 Elsevier Science (USA). All rights reserved.
doi:10.1016/S1090-7807(03)00003-X

2. Optimal control of nuclear spins under relaxation

The various relaxation mechanisms in NMR spectroscopy have been well studied [1,3]. In liquid solutions, the most important relaxation mechanisms are due to dipole–dipole interaction (DD) and chemical shift anisotropy (CSA), as well as their interference effects (e.g. DD-CSA cross-correlation terms) [4]. The optimal control methodology presented here is very general and can take into account arbitrary relaxation mechanisms. To demonstrate the ideas and basic principles we focus on an isolated pair of heteronuclear spins I (e.g., ^{1}H) and S (e.g., ^{3}C or ^{15}N) with a scalar coupling J. Both spins are assumed to be on resonance in a doubly rotating frame and only dipole–dipole and CSA relaxation is considered (no cross-correlated relaxation). This case approximates for example the situation for deuterated and ^{15}N-labeled proteins in H_2O where ^{1}H–^{15}N spin pairs are isolated. In particular, we focus on slowly tumbling molecules in the spin diffusion limit [1]. In this case longitudinal relaxation rates are negligible compared to transverse relaxation rates [1].

For such coupled two-spin systems, the quantum mechanical equation of motion (Liouville–von Neumann equation) for the density operator ρ [1] is given by

$$\dot{\rho} = \pi J[-\mathrm{i}2I_zS_z, \rho] + \pi k_{\mathrm{DD}}[2I_zS_z, [2I_zS_z, \rho]] + \pi k^I_{\mathrm{CSA}}[I_z[I_z, \rho]] + \pi k^S_{\mathrm{CSA}}[S_z, [S_z, \rho]]. \quad (1)$$

Here J is the scalar coupling constant and k_{DD} is the transverse relaxation rate due to dipole–dipole relaxation. The k^I_{CSA} and k^S_{CSA} represents the CSA relaxation rate for spin I and S, respectively. The net transverse relaxation rate for spin I and S is denoted by k^I and k^S, respectively, and is given by

$$k^I = k_{\mathrm{DD}} + k^I_{\mathrm{CSA}}, \quad k^S = k_{\mathrm{DD}} + k^S_{\mathrm{CSA}}.$$

These relaxation rates depend on various physical parameters, such as the gyromagnetic ratios of the spins, the internuclear distance, and the correlation time of the molecular tumbling [1]. In this paper, we address the problem of finding the maximum efficiency for the transfers

$$I_\alpha \rightarrow 2I_\beta S_\gamma \quad (2)$$

and

$$I_\alpha \rightarrow S_\beta, \quad (3)$$

where α, β, and γ can be x, y, or z. These transfers are of central importance for two-dimensional NMR spectroscopy and are conventionally accomplished by the insensitive nuclei enhanced by polarization transfer (INEPT) [5] (see Fig. 1a) and refocused INEPT [6] pulse sequence elements, respectively.

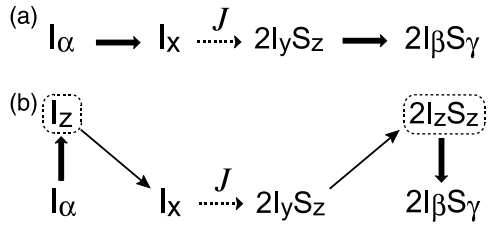

Fig. 1. Transfer schemes for (a) INEPT and (b) ROPE (Relaxation Optimized Pulse Element) for the transfer $I_\alpha \rightarrow 2I_\beta S_\gamma$. Thick and thin arrows represent selective spin rotations by strong and weak rf pulses, respectively. Dashed arrows represent evolution under J couplings.

The two heteronuclear spins have well separated resonance frequencies, allowing for fast selective manipulation of each spin on a time-scale determined by the coupling J and the relaxation rates. Hence, in the following it is assumed that any initial Cartesian spin operator I_α can be transformed to an operator of the form $I_x \cos\beta_1 + I_z \sin\beta_1$ by the use of strong, spin-selective radio frequency (rf) pulses without relaxation losses (see Fig. 2). Let $r_1(t)$ represent the magnitude of polarization and in-phase coherence on spin I at any given time t, i.e. $r_1^2(t) = \langle I_x\rangle^2 + \langle I_z\rangle^2$, where $\langle I_\alpha\rangle = \mathrm{trace}\{\rho I_\alpha\}$ represents the expectation value of I_α. Using rf fields, we can exactly control the angle β_1 in the term $r_1(t)\sin\beta_1 I_z + r_1(t)\cos\beta_1 I_x$. Hence we can think of $\cos\beta_1$ as a control parameter and denote it by u_1 (see Fig. 2).

Observe that the operator I_z is invariant under the evolution Eq. (1), whereas I_x evolves under the J coupling to $2I_yS_z$ and also relaxes with rate k^I. As the operator $2I_yS_z$ is produced, it also relaxes with rate k^I. By use of rf pulses it is possible to rotate the coherence operator $2I_yS_z$ to $2I_zS_z$, which is protected from relaxation (see Fig. 1b). Let r_2 represent the total magnitude of the expectation values of these bilinear operators, i.e. $r_2^2(t) = \langle 2I_yS_z\rangle^2 + \langle 2I_zS_z\rangle^2$. We can control the angle β_2 in the term $r_2(t)\cos\beta_2 2I_yS_z + r_2(t)\sin\beta_2 2I_zS_z$ and we define $\cos\beta_2$ as a second control parameter u_2 (see Fig. 2). The evolution of $r_1(t)$ and $r_2(t)$ under the scalar coupling and relaxation can be expressed as follows.

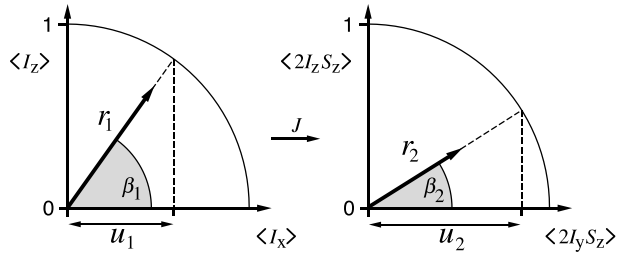

Fig. 2. Representation of the system variables r_1, r_2, the angles β_1, β_2, and of the control parameters $u_1 = \cos\beta_1$, $u_2 = \cos\beta_2$ in terms of the expectation values $\langle I_x\rangle$, $\langle I_z\rangle$, $\langle 2I_yS_z\rangle$, and $\langle 2I_zS_z\rangle$.

From Eq. (1), we have

$$\frac{d\langle I_z\rangle(t)}{dt} = 0,$$
$$\frac{d\langle I_x\rangle(t)}{dt} = -\pi J\langle 2I_yS_z\rangle(t) - \pi k^I\langle I_x\rangle(t),$$
$$\frac{d\langle 2I_zS_z\rangle(t)}{dt} = 0,$$
$$\frac{d\langle 2I_yS_z\rangle(t)}{dt} = \pi J\langle I_x\rangle(t) - \pi k^I\langle 2I_ys_z\rangle(t).$$

Using the fact that $r_1(t) = \sqrt{\langle I_z\rangle^2(t) + \langle I_x\rangle^2(t)}$ and $r_2(t) = \sqrt{\langle 2I_yS_z\rangle^2(t) + \langle 2I_zS_z\rangle^2(t)}$ and above set of equations, we can write

$$\frac{d}{dt}\begin{bmatrix} r_1(t) \\ r_2(t)\end{bmatrix} = \pi J\begin{bmatrix} -(k^I/J)\cos^2\beta_1(t) - \cos\beta_1(t)\cos\beta_2(t) \\ \cos\beta_1(t)\cos\beta_2(t) - (k^I/J)\cos^2\beta_2(t)\end{bmatrix} \times \begin{bmatrix} r_1(t) \\ r_2(t)\end{bmatrix}.$$

Using $u_1 = \cos\beta_1$ and $u_2 = \cos\beta_2$, we get

$$\frac{d}{dt}\begin{bmatrix} r_1(t) \\ r_2(t)\end{bmatrix} = \pi J\begin{bmatrix} -\xi u_1^2 & -u_1u_2 \\ u_1u_2 & -\xi u_2^2\end{bmatrix}\begin{bmatrix} r_1(t) \\ r_2(t)\end{bmatrix}. \quad (4)$$

Here

$$\xi = k^I/J \quad (5)$$

is the relative relaxation rate and measures the relative strength of the relaxation rate k^I to the spin–spin coupling J.

The central problem addressed in this paper is the following: Given the dynamical system in Eq. (4), how should $u_1(t)$ and $u_2(t)$ be chosen so that starting from $r_1(0) = 1$ we achieve the largest value for r_2. In spectroscopic applications this would correspond to the maximum efficiency for the transfer of I_α to $2I_\beta S_\gamma$ (Eq. (2)). Observe if $\xi = 0$ (no relaxation), then by putting $u_1(t) = u_2(t) = 1$, we have $r_2(1/2J) = 1$, i.e. after a time $t = 1/2J$ the operator I_x is completely transferred to $2I_yS_z$. This is the INEPT transfer element [5]. However if $\xi > 0$, it is not the best strategy to keep $u_1(t)$ and $u_2(t)$ both 1 (as demonstrated subsequently), see Fig. 3a. Using principles of optimal control theory, it is possible to obtain analytical expressions for the largest achievable value of r_2 and the optimal values of $u_1(t)$ and $u_2(t)$, see solid curve in Fig. 3a. One of the main results of the paper is as follows.

For the dynamical system in Eq. (4) the maximum achievable value of r_2 (i.e., the maximum transfer efficiency η) is given by

$$\eta = \sqrt{1+\xi^2} - \xi \quad (6)$$

and the optimal controls $u_1^*(t)$ and $u_2^*(t)$ satisfy the relation

$$\frac{u_2^*(t)}{u_1^*(t)} = \eta\frac{r_1(t)}{r_2(t)}. \quad (7)$$

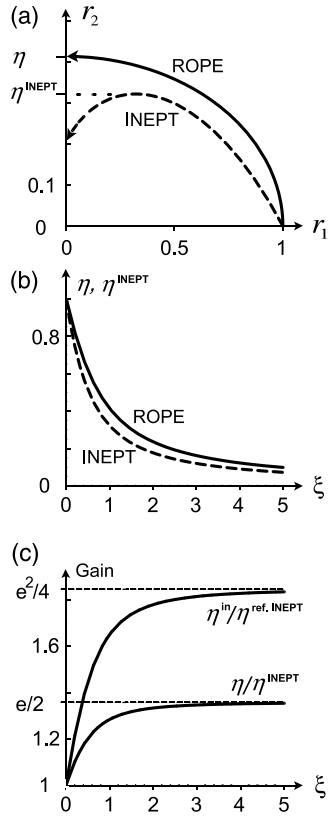

Fig. 3. (a) The dashed curve shows the trajectory of the dynamical system (4) when $\xi = 1$ and $u_1(t)$ and $u_2(t)$ are maintained at value 1 (INEPT transfer). The maximum transfer amplitude η^{INEPT} is reached at $t^* = (4J)^{-1}$. The solid curve represents the trajectory for optimal choice of $u_1(t)$ and $u_2(t)$ (ROPE transfer). (b) Efficiency η^{INEPT} of INEPT (dashed curve) and efficiency η of ROPE (solid curve) as a function of the relative relaxation rate ξ for transfer (2). (c) Gain of ROPE transfer efficiency compared to INEPT-type experiments for transfer (2) ($\eta/\eta^{\mathrm{INEPT}}$) and for the in-phase transfer (3) ($\eta^{\mathrm{in}}/\eta^{\mathrm{ref.INEPT}}$).

This implies that throughout the optimal transfer process, the ratio of $\langle 2I_yS_z\rangle(t)$ and $\langle I_x\rangle(t)$ is always maintained at (see Fig. 4)

$$\frac{\langle 2I_yS_z\rangle(t)}{\langle I_x\rangle(t)} = \eta. \quad (8)$$

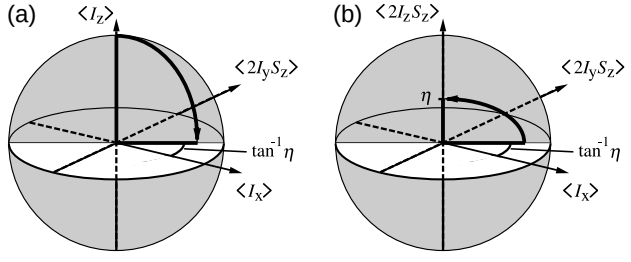

Fig. 4. Schematic representation of the relation (8) to be satisfied by the optimal trajectory. (a) In the first period during which $\langle I_z\rangle > 0$, the density operator ρ is restricted to the three-dimensional subspace spanned by the operators I_x, $2I_yS_z$, and I_z. (b) In the next period during which $\langle I_z\rangle = 0$, the density operator ρ is restricted to the three-dimensional subspace spanned by the operators I_x, $2I_yS_z$, and $2I_zS_z$. The optimal trajectory lies in the plane which satisfies Eq. (8).

The optimality of this choice of u_1 and u_2 can intuitively be established as follows. As r_1 is transferred to r_2, the ratio r_2/r_1 increases from 0 to ∞. The choice of optimal u_1 and u_2 should be such that the ratio of gain δr_2 in r_2 to loss δr_1 in r_1 for incremental time steps δt is maximized. If we compute this ratio, we get

$$\frac{\dot{r_2}}{-\dot{r_1}} = \frac{r_1}{r_2}\frac{p-\xi p^2}{p+\xi},$$

where $p = (u_2 r_2)/(u_1 r_1)$. If we maximize the above expression with respect to p for a given r_2/r_1 we get the optimal $p^* = \eta$. Implying the optimal controls $u_1^*(t)$ and $u_2^*(t)$ satisfy the relation (7).

Experimentally, the relaxation optimized pulse element (ROPE) which achieves this optimal efficiency has the following characterization. Starting from the coherence operator I_x ($r_1 = 1$, $r_2 = 0$), this operator is immediately transformed to the polarization operator I_z (which is protected against relaxation). Then the operator I_z is gradually rotated towards I_x (which relaxes and also evolves to $2I_yS_z$ under the coupling term) such that Eq. (8) is fulfilled for all times. Once $\langle I_z\rangle$ becomes 0, the operator $2I_yS_z$ is gradually rotated to $2I_zS_z$ (which is also protected against relaxation), again maintaining the relation of Eq. (8) (see Fig. 4). Finally, $2I_zS_z$ is rapidly rotated to the target state $2I_\beta S_\gamma$ (see Fig. 1b).

It is instructive to compare the optimum coherence transfer efficiency η (Eq. (6)) for the ROPE transfer (solid curve in Fig. 3b) with the maximum transfer efficiency of INEPT. Recall, in INEPT, the efficiency of the transfer $I_x \to 2I_zS_y$ as a function of transfer time t is given by $\eta^{\mathrm{INEPT}}(t) = \exp(-\pi k t)\sin(\pi J t)$. This efficiency is maximized for a transfer time $t^* = (1/\pi J)\cot^{-1}(\xi)$ and this value is $\eta^{\mathrm{INEPT}}(t^*) = \exp(-\xi\cot^{-1}(\xi))\sin(\cot^{-1}(\xi))$. Fig. 3c shows the ratio $\eta/\eta^{\mathrm{INEPT}}$ as a function of ξ. In the limit $\xi \gg 1$ the ratio $\eta/\eta^{\mathrm{INEPT}}$ approaches $e/2 = 1.359$.

For the transfer $I_x \to S_x$ (3) the operator I_x is first transferred to $2I_zS_y$ which is then transformed to S_x. The optimal transfer $2I_zS_y \to S_x$ has similar character as the optimal transfer $I_x \to 2I_zS_y$ and has the transfer efficiency given by $\sqrt{1+(k^S/J)^2} - (k^S/J)$. Therefore, the total efficiency for the in-phase to in-phase ROPE transfer is

$$\eta^{\mathrm{in}} = \left(\sqrt{1+\left(\frac{k^I}{J}\right)^2} - \frac{k^I}{J}\right)\left(\sqrt{1+\left(\frac{k^S}{J}\right)^2} - \frac{k^S}{J}\right).$$

If $k^I = k^S$, then $\eta^{\mathrm{in}} = \eta^2$. Fig. 3c also shows the ratio of this optimal efficiency versus the maximum efficiency of the refocused INEPT sequence $\eta^{\mathrm{ref.INEPT}} = (\eta^{\mathrm{INEPT}})^2$ for the case when $k^I = k^S$. In the limit of large ξ, the ratio approaches $e^2/4 = 1.847$, i.e., gains of nearly 85% are possible using relaxation optimized pulse elements (ROPE).

The formal proof of the above results is based on the central tenet of optimal control theory, the principle of dynamic programming [7]. In this framework, to find the optimal way to steer system (4) from the starting point $(r_1, r_2) = (1, 0)$ to the largest possible value r_2, we need to find the best way to steer this system for all choices of the starting points (r_1, r_2). Starting from (r_1, r_2), we denote the maximum achievable value of r_2 by $V(r_1, r_2)$, also called the optimal return function for the point (r_1, r_2). The optimal return function for system (4) and optimal control $u_1(r_1, r_2)$ and $u_2(r_1, r_2)$ satisfy the well known Hamilton Jacobi Bellman equation, see Appendix A for details. It is shown in Appendix A that the optimal return function for the control system (4) is

$$V(r_1, r_2) = \sqrt{\eta^2 r_1^2 + r_2^2} \tag{9}$$

and the optimal controls satisfy Eq. (7). Evaluating the optimal return function at $(1, 0)$, we get $V(1, 0) = \eta$. Therefore, the maximum transfer efficiency in a spectroscopy experiment involving transfer of polarization I_x to $2I_zS_x$ is η and the optimal controls u_1 and u_2 satisfy Eq. (7).

It is important to note that in the above problem, there is no constraint on the the time required to transfer I_x to $2I_zS_x$. The maximum achievable efficiency obtained as a solution to the above problem can only be achieved in the limit of very long transfer times (although most of the efficiency in achieved in finite time). In practice, it is desirable to reduce the duration of the pulse sequence. Therefore this raises the question, what is the maximum transfer efficiency of I_α to $2I_\beta S_\gamma$ in a given finite time T. This problem can also be explicitly solved (see Appendix B). Here, we describe the characteristics of the optimal pulse sequence: If $T \leqslant (\cot^{-1}(2\xi))/\pi J$, then $u_1(t) = u_2(t) = 1$ throughout, i.e., β_1 and β_2 in Fig. 2 are always kept zero. This solution corresponds to the INEPT pulse sequence. For $T > (\cot^{-1}(2\xi))/\pi J$ the optimal trajectory has three distinct phases (see Figs. 5 and 6).

There is a τ (which is a function of T), such that for $0 \leqslant t \leqslant \tau$ (phase I), $u_2(t) = 1$ and $u_1(t)$ is increased gradually from a value $u_1(0) < 1$ to $u_1(\tau) = 1$ (see Appendix B). Then for time $\tau \leqslant t \leqslant T - \tau$ (phase II), the optimal control $u_1(t) = u_2(t) = 1$. Finally for $t \geqslant T - \tau$ (phase III), we have $u_1(t) = 1$ and $u_2(t)$ is decreased from $u_1(T - t) = 1$ to $u_2(T) = u_1(0)$. The optimal control always satisfies $u_1(t) = u_2(T - t)$, as depicted in Fig. 6a. The parameter τ is related to T through the following equation:

$$T = 2\tau + \frac{\theta_2 - \theta_1}{\pi J}, \tag{10}$$

where

$$\theta_1 = \cot^{-1}\frac{1-\kappa(\tau)}{2\xi\kappa(\tau)}, \quad \theta_2 = \tan^{-1}\frac{1-\kappa(\tau)}{2\xi},$$

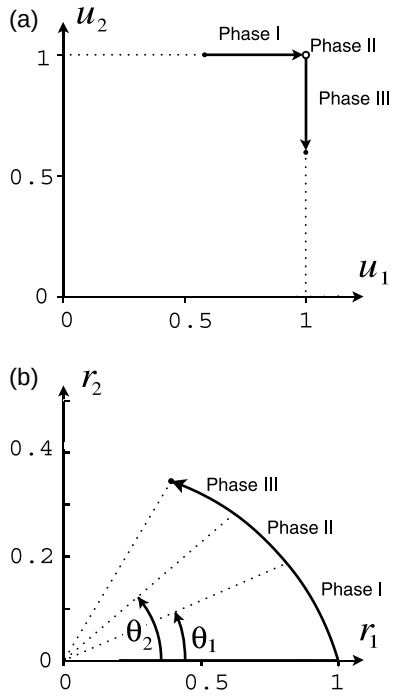

Fig. 5. Phase trajectory of the controls u_1 and u_2 (panel a) and $\vec{r}(t)$ (panel b) for a finite-time ROPE sequence ($\xi = 1$).

$$\kappa(\tau) = 1 + 2\xi^2 - 2\xi\sqrt{1+\xi^2}\coth\left(\pi J\sqrt{1+\xi^2}\tau + 2\sinh^{-1}\xi\right).$$

At time τ, the optimal trajectory (r_1, r_2) passes from phase I to II and makes an angle θ_1 with the r_1 axis and at time $T-\tau$ the optimal trajectory passes from phase II to phase III and makes an angle θ_2 with the r_1 axis (see Fig. 5b). The optimal efficiency η_T for the finite time T is expressed in terms of these angles as

$$\eta_T = \frac{\exp(\xi(\theta_1-\theta_2))(1-\xi\sin 2\theta_2)}{\sin(\theta_1+\theta_2)}. \tag{11}$$

In the limit, T goes to infinity $\tau = T/2$ and $\theta_1 = \theta_2 = \tan^{-1}\sqrt{1+\xi^2} - \xi$ and η_T approaches η in (6). This corresponds to the unconstrained time case we discussed initially. For the general finite time problem, we can analytically characterize the optimal controls (see Fig. 6a) and the optimal rf pulse elements (see Fig. 6b) as following.

For $0 \leqslant t \leqslant \tau$, the optimal control is given by

$$u_1(t) = \sqrt{\frac{R_1^2\{1+\cosh(\phi(t))\}}{(BR_1^2 + 2A^2R_2^2) - R_1^2\cosh(\phi(t))}},$$

where $A = \sinh\phi(\tau/2)$, $B = \cosh\phi(\tau)$, and $\phi(t) = 2\sinh^{-1}\xi + 2\pi Jt\sqrt{1+\xi^2}$. The optimal trajectory crosses from region II to region III at the point

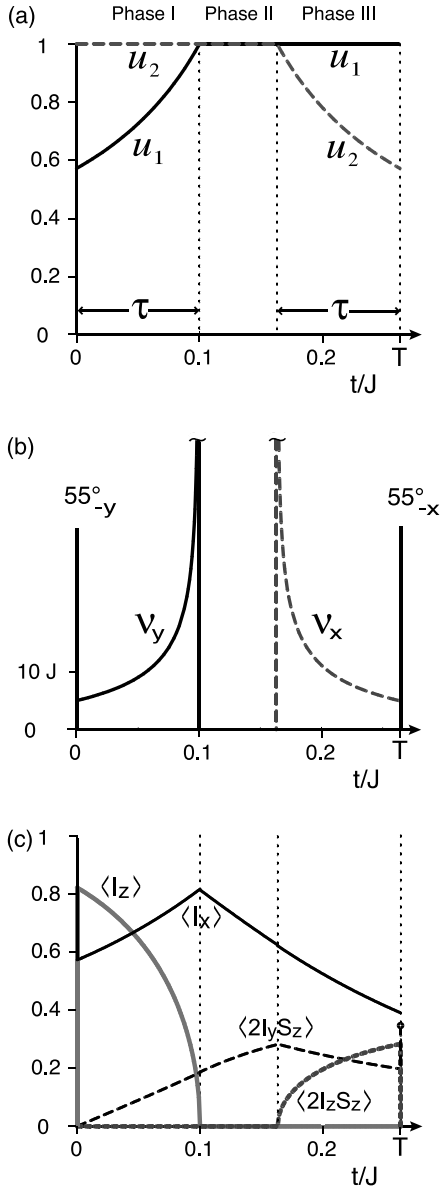

Fig. 6. Controls u_1 and u_2 (panel a), the corresponding rf pulse sequence (panel b) and the expectation values $\langle I_z\rangle$, $\langle I_x\rangle$, $\langle 2I_yS_z\rangle$, and $\langle 2I_zS_z\rangle$ (panel c) are shown for a finite-time ROPE sequence ($\xi = 1$, $\tau = 0.1J^{-1}$, $T = 0.263J^{-1}$) that optimizes the transfer $I_x \to 2I_yS_z$. In panel b, the initial hard $55_{-y}°$ pulse establishes $u_1(0) = 0.572$ (see panel a) and the final hard $55_{-x}°$ pulse completes the transfer. During phase I and III, the optimal rf amplitudes $B_{x,y}^{\mathrm{rf}}(t)$ are given in frequency units ($\nu_{x,y}(t) = \gamma_I B_{x,y}^{\mathrm{rf}}(t)/2\pi$, where γ_I is the gyromagnetic ratio of spin I). During phase II no rf pulses are applied. Approaching phase II (Panel b) the rf amplitude becomes large for a very short time period. This can experimentally be very well approximated by a hard pulse of small flip angle.

$$(R_1, R_2) = \left(\frac{\eta_T}{\sqrt{\tan^2\theta_2 + \kappa(\tau)}}, \frac{\eta_T}{\sqrt{1+(\kappa(\tau)/\tan^2\theta_2)}}\right)$$

(as depicted in Fig. 5). For $t > \tau$, we have $u_1(t) = 1$ and $u_2(t) = u_1(T-t)$. The explicit expression for the rf-amplitude v_y for phase I in panel b of Fig. 6 in terms of u_1 is

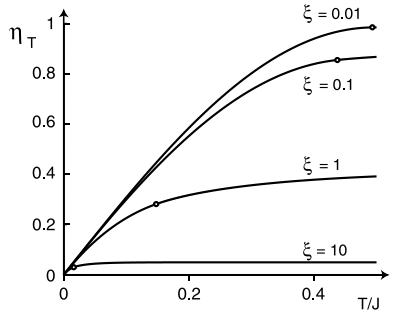

Fig. 7. Optimal transfer efficiency η_T as a function of the total transfer time T for various values of ξ. The circles indicate the critical time $\frac{\cot^{-1}(2\xi)}{\pi J}$ below which the ROPE sequences are identical to the standard INEPT sequence. For times greater than this critical time, the ROPE sequences are more efficient than INEPT.

$$v_y(t) = 2\pi J \frac{u_1}{\sqrt{1-u_1^2}} \tanh\left(\frac{\phi}{2}\right)\sqrt{1+\xi^2},$$

and in phase III, $v_x(t) = v_y(T-t)$. For the transfer $I_z \rightarrow 2I_zS_z$, the flip angle of the initial and final hard pulses (see Fig. 6b) is given by $\sin^{-1} u_1(0)$. For $\xi = 1$ and $T = (0.263/J)$ we find $u_1(0) = 0.5716$. The resulting value for initial and final flip angle is 55.138°.

Fig. 7 depicts the maximum achievable efficiency as a function of transfer time T for various values of ξ.

3. Experimental

Experimental tests were performed using ^{3}C-labeled sodium formate dissolved in 92% D_6–glycerol and 8% D_2O as a heteronuclear model two-spin system with $J = 193$ Hz, where ^{1}H and ^{3}C represent spins I and S, respectively. At a temperature of 250 K, and a proton frequency of 500 MHz, the transverse relaxation time T_2 of spin I was 1.4 ms, corresponding to a rate $k^I = (\pi T_2)^{-1} = 227$ Hz, corresponding to $\xi = k^I/J = 1.18$. At this field strength the transverse relaxation of the protons is dominated by the dipolar relaxation mechanism. In the preparation phase of the experiments, the thermal equilibrium S magnetization was dephased by applying a 90° (S) pulse followed by a pulsed magnetic field gradient. The transfer of $I_z \rightarrow 2I_zS_z$ was effected by INEPT and ROPE experiments. Finally, a hard 90° (S) pulse was applied to transform $2I_zS_z$ to $2I_zS_y$. The relative transfer efficiencies were determined by comparing the resulting anti-phase signals of spin S (see Fig. 8). Both INEPT and ROPE sequences were performed without the use of refocussing pulses and both spins I and S were irradiated on resonance. For INEPT, the maximum transfer efficiency was found for a duration of 1.2 ms (gray curve in Fig. 8). A ROPE sequence with a total duration of $T = 5.006$ ms and a duration $\tau = 2.5$ ms of phase I (and of phase III) was used. The

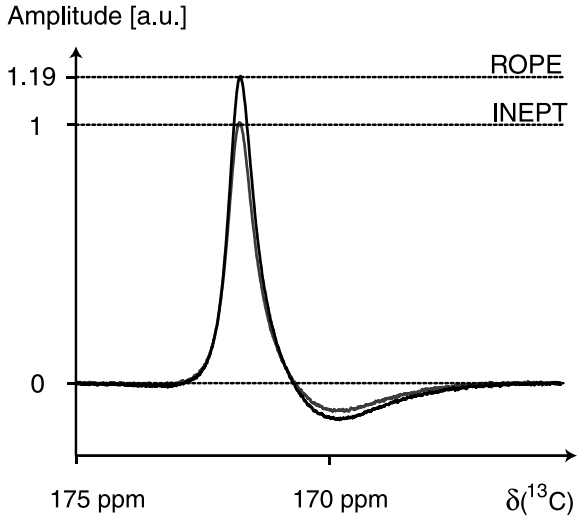

Fig. 8. Experimental antiphase signal $2I_zS_y$ after INEPT (gray curve) and ROPE (black curve) transfer of $I_z \rightarrow 2I_zS_z$, followed by a hard 90° (S) pulse. Spins I and S correspond to the ^{1}H–^{3}C spins of ^{3}C-labeled sodium formate in in 92% D_6-glycerol and 8% D_2O at a temperature of 250 K.

hard and shaped pulse (see Fig. 6b) of phase I was approximated by a series of equally spaced 8 hard pulses with flip angles 4.4°, 2.5°, 3.6°, 5.3°, 7.7°, 11.6°, 19.1°, 62.5°, and rf amplitude of 2.5 kHz. Similarly, the shaped and hard pulse of phase III was approximated by a series of equally spaced 8 hard pulses with flip angles 0°, 54°, 21.6°, 13.5°, 9°, 6.1°, 4.2°, and 4.4°. For $\xi = 1.17$, a gain of 29.9% is expected for an ideal ROPE sequence compared to INEPT. For the finite time implementation with $T = 5.006$ ms with only 8 hard pulses in phase I and III, a gain of 27% is expected according to numerical simulations. Experimentally, a gain of 19% was found. The discrepancy between the theoretical and experimental gain can be attributed to non-vanishing cross-correlation effects, experimental imperfections such as rf inhomogeneity and non-vanishing longitudinal relaxation rates. However, the superior transfer characteristics of the ROPE transfer scheme has clearly been demonstrated by the experiment.

4. Conclusions and outlook

In this paper, we initiated the study of a new class of control systems which arise naturally in optimal control of quantum mechanical systems in the presence of relaxation. This made it possible to derive for the first time upper achievable physical limits on the efficiency of coherence and polarization transfer on two-coupled spins. In this paper, the focus was on the study of an isolated pair of scalar coupled heteronuclear spins under dipole–dipole and CSA relaxation in the spin diffusion

limit. For this example a surprising new transfer scheme was found which yields substantial gains (of up to 85%) in transfer efficiency. The methods presented here are by no means limited to the case of coupled two spins. These can be generalized for finding relaxation optimized pulse sequences in larger spin systems as commonly encountered in backbone and side chain assignments in protein NMR spectroscopy. Furthermore these methods directly extend to other routinely used experiments like excitation of multiple quantum coherence [1]. Some obvious extensions of the methodology presented here are to incorporate cross-correlation effects [4] among different relaxation mechanisms and to include in the design of pulse sequences additional criteria such as broadbandedness and robustness with respect to relaxation rates and experimental imperfections. The methods presented here are not restricted to NMR applications but are broadly applicable to coherent control of quantum-mechanical phenomena in the presence of dissipation and decoherence. The control systems studied in this paper are characterized by the fact that they are linear in the state of the system and controls can be expressed as polynomial functions of fewer parameters. Such systems have so far not received much attention in the optimal control literature due to lack of physical motivation. It is expected that the study of these systems will foster further developments in the area of system science and mathematical control theory.

Acknowledgments

N.K. acknowledges Darpa Grant F49620-01-1-0556 and NSF Grants ECS-0133673 for their support. S.J.G. acknowledges support from Fonds der Chemischen Industrie and the Deutsche Forschungsgemeinschaft for Grant Gl 203/4-1. B.L. acknowledges support from Fonds der Chemischen Industrie and the Deutsche Forschungsgemeinschaft (Emmy Noether-Stipend Lu 835/1-1). The authors thank Dionisis Stefanatos for proof reading the manuscript.

Appendix A. Optimal coherence transfer with no time constraint

If we start at (r_1, r_2), then by making a choice of controls in (4) and letting the dynamical system evolve, after small time δt we can make a transition to all points $(\tilde{r}_1, \tilde{r}_2)$, which are related to (r_1, r_2), by

$$\begin{bmatrix} \tilde{r}_1 \\ \tilde{r}_2 \end{bmatrix} = \begin{bmatrix} r_1 \\ r_2 \end{bmatrix} + \delta t \pi J \begin{bmatrix} -\xi u_1^2 & -u_1 u_2 \\ u_1 u_2 & -\xi u_2^2 \end{bmatrix} \begin{bmatrix} r_1 \\ r_2 \end{bmatrix}.$$

From all points $(\tilde{r}_1, \tilde{r}_2)$ that can be reached by appropriate choice of (u_1, u_2) in small time δt, we should choose to go to that $(\tilde{r}_1, \tilde{r}_2)$ for which $V(\tilde{r}_1, \tilde{r}_2)$ is the largest. But now note by definition of V that $V(r_1, r_2) = \max_{\tilde{r}_1, \tilde{r}_2} V(\tilde{r}_1, \tilde{r}_2)$. This can be re-written as

$$V(r_1, r_2) = \max_{u_1, u_2} V(r_1 + \delta t(-\xi u_1^2 r_1 - u_1 u_2 r_2), r_2 + \delta t(-\xi u_2^2 r_2 + u_1 u_2 r_1))$$

for infinitesimal δt. The right-hand side of the above expression can be expanded (Taylor series expansion) in powers of δt and retaining only the terms linear in δt (for δt approaching zero), we get

$$V(r_1, r_2) = V(r_1, r_2) + \delta t \pi J \times \max_{u_1, u_2} \begin{bmatrix} \frac{\partial V}{\partial r_1} & \frac{\partial V}{\partial r_2} \end{bmatrix} \begin{bmatrix} -\xi u_1^2 & -u_1 u_2 \\ u_1 u_2 & -\xi u_2^2 \end{bmatrix} \begin{bmatrix} r_1 \\ r_2 \end{bmatrix}.$$

Let

$$\mathbb{H} = \begin{bmatrix} \frac{\partial V}{\partial r_1} & \frac{\partial V}{\partial r_2} \end{bmatrix} \begin{bmatrix} -\xi u^2 & -uv \\ uv & -\xi v^2 \end{bmatrix} \begin{bmatrix} r_1 \\ r_2 \end{bmatrix}.$$

This equation then reduces to

$$\max_{u_1, u_2} \mathbb{H}(u_1, u_2) = 0. \tag{A.1}$$

The optimal control $u_1(r_1, r_2)$ and $u_2(r_1, r_2)$ maximizes the above expression and its maximum value is zero. If we can find a function $V(r_1, r_2)$, which satisfies Eq. (A.1) then finding (u_1, u_2) which satisfy (A.1) will give us the optimal control to apply in any given state of the dynamical system.

Let $\mathbb{H}(u_1, u_2)$ be as above. Let $\lambda_1 = (\partial V/\partial r_1)$, $\lambda_2 = (\partial V/\partial r_2)$, $a = (\lambda_2/\lambda_1)$, and $b = (r_2/r_1)$. Then

$$\mathbb{H} = -\lambda_1 r_1 [\xi a b u_2^2 + (b - a) u_1 u_2 + \xi u_1^2].$$

Observe if $(a - b) \leqslant 0$, then the only solution to Eq. (A.1) is the trivial solution $u_1^* = u_2^* = 0$. Therefore $(a - b) > 0$. Also note, when $(a - b)^2 < 4\xi^2 ab$, the only solution to Eq. (A.1) is again the trivial solution. Therefore the only case for which (A.1) can be satisfied is if $(b - a)^2 = 4ab\xi^2$, implying $\sqrt{(b/a)} = \sqrt{1 + \xi^2} - \xi$. In this regime, maximizing $\mathbb{H}$, we get $(u_1^*/u_2^*) = (a - b)/2\xi$ implying $(u_1^*/u_2^*) = (b/\sqrt{1 + \xi^2} - \xi)$. Integrating Eq. (4), for this choice of optimal control, we get that starting from the point (r_1, r_2), the optimal trajectory satisfies that $r_2(t)$ approaches $\sqrt{\eta^2 r_1^2 + r_2^2}$ for large t. This is then the desired optimal return function $V(r_1, r_2)$. It can be verified that the optimal return function satisfies Eq. (A.1).

Appendix B. Finite time case

We rescale time to eliminate the factor πJ in Eq. (4). Rewriting (4) in new time units we get

$$\frac{\mathrm{d}}{\mathrm{d}t} \begin{bmatrix} r_1(t) \\ r_2(t) \end{bmatrix} = \begin{bmatrix} -\xi u_1^2 & -u_1 u_2 \\ u_1 u_2 & -\xi u_2^2 \end{bmatrix} \begin{bmatrix} r_1(t) \\ r_2(t) \end{bmatrix}. \tag{B.1}$$

In the finite time case, the optimal return function $V(r_1, r_2, t)$ has explicit dependence on time and by definition

$$V(r_1, r_2, t) = \max_{u_1,u_2} V(r_1 + \delta t(-\xi u_1^2 r_1 - u_1 u_2 r_2), r_2 + \delta t(-\xi u_2^2 r_2 + u_1 u_2 r_1), t + \delta t).$$

Expanding again in powers of δt , we obtain the well known Hamilton Jacobi Bellman equation [7]

$$\frac{\partial V}{\partial t} + \max_{u_1,u_2} \begin{bmatrix} \frac{\partial V}{\partial r_1} & \frac{\partial V}{\partial r_2} \end{bmatrix} \begin{bmatrix} -\xi u_1^2 & -u_1 u_2 \\ u_1 u_2 & -\xi u_2^2 \end{bmatrix} \begin{bmatrix} r_1 \\ r_2 \end{bmatrix} = 0. \quad \text{(B.2)}$$

As in Appendix A, let $\mathbb{H} = -\lambda_1 r_1[\xi u_1^2 - (a-b)\ u_1 u_2 + \xi a b u_2^2]$. Then Eq. (B.2) can be rewritten as

$$\frac{\partial V}{\partial t} + \max_{u_1,u_2} \mathbb{H}(u_1, u_2) = 0.$$

For the finite time problem $\max_{u_1,u_2} \mathbb{H} > 0$. This implies $(a-b)^2 > 4\xi^2 ab$. We consider three separate cases for the problem

1. *Case* I: If $(a-b) < 2\xi$, then the maximum of $\mathbb{H}$ is obtained for $u_2 = 1$ and $u_1 = (a-b)/2\xi$.
2. *Case* II: If $(a-b) \geqslant 2\xi$ and $(a-b)/ab \geqslant 2\xi$, then the maximum of $\mathbb{H}$ is obtained for $u_1 = 1$ and $u_2 = 1$.
3. *Case* III: If $(a-b)/ab < 2\xi$, then the maximum of $\mathbb{H}$ is obtained for $u_1 = 1$ and $u_2 = (a-b)/2\xi ab$.

From Eq. (B.2), the adjoint variables $(\lambda_1, \lambda_2) = (\partial V/\partial r_1, \partial V/\partial r_2)$ satisfy the equations $\dot{\lambda}_1 = -(\partial \mathbb{H}/\partial r_1)$ and $\dot{\lambda}_2 = -(\partial \mathbb{H}/\partial r_2)$, i.e.

$$\frac{\mathrm{d}}{\mathrm{d}t} \begin{bmatrix} \lambda_1 \\ \lambda_2 \end{bmatrix} = \begin{bmatrix} \xi u_1^2 & -u_1 u_2 \\ u_1 u_2 & \xi u_2^2 \end{bmatrix} \begin{bmatrix} \lambda_1 \\ \lambda_2 \end{bmatrix}, \quad \text{(B.3)}$$

where $(\lambda_1(T), \lambda_2(T)) = (0, 1)$. From Eqs. (B.1) and (B.3), we deduce that $V = \lambda_1 r_1 + \lambda_2 r_2$ is a constant for optimal trajectory and equals the optimal cost $r_2(T) = \lambda_1(0)$. Writing the equation for adjoint variables backward in time, let $\sigma = T - t$ then

$$\frac{\mathrm{d}}{\mathrm{d}\sigma} \begin{bmatrix} \lambda_1 \\ \lambda_2 \end{bmatrix} = \begin{bmatrix} -\xi u_1^2 & u_1 u_2 \\ -u_1 u_2 & -\xi u_2^2 \end{bmatrix} \begin{bmatrix} \lambda_1 \\ \lambda_2 \end{bmatrix},$$

where $(\lambda_1(\sigma), \lambda_2(\sigma))_{\sigma=0} = (0, 1)$. Now $u_1(\sigma)$ and $u_2(\sigma)$ should be chosen to maximize $\lambda_1(\sigma)|_{\sigma=T}$. Observe this is exactly the same optimization problem as (B.1), where the roles of u_1 and u_2 have been switched. From the symmetry of these two optimization problems, we then have

$$u_1^*(t) = u_2^*(T-t),$$
$$r_1(t) = \lambda_2(T-t); \quad r_2(t) = \lambda_1(T-t),$$
$$ab\left(\frac{T}{2}\right) = 1; \quad V = 2r_1\left(\frac{T}{2}\right) r_2\left(\frac{T}{2}\right).$$

Observe from (B.1) and (B.3), that $ab(t)$ is monotonically increasing and since $ab(0) = 0$ and $ab(T/2) = 1$, we have $ab(t) < 1$ for $t < T/2$. Therefore $u_2^*(t) = 1$ for $t < T/2$. Since $b(0) = 0$, depending on $a(0)$ we have two cases. *Case* A: In this case $a(0)/2\xi \geqslant 1$. Then we start in the case II discussed above and verify that in this case $a - b$ is increasing for $ab < 1$. Therefore we stay in this case for all $t \in [0, T/2]$ and therefore $u_1^* = u_2^*(t) = 1$ for all t. Since $b(0) = 0$, we have $b(T/2) = \tan T$. Similarly,

$$a\left(\frac{T}{2}\right) = \frac{a(0) + \tan\left(\frac{T}{2}\right)}{1 - a(0)\tan\left(\frac{T}{2}\right)}.$$

If $ab(T/2) = 1$. then above equation implies that $\tan(T) \leqslant 1/2\xi$.

Case B. If $a(0)/2\xi < 1$, then $u_1^*(0) = a(0)/2\xi$ and the system begins in case I. Let $\kappa(t)$ satisfy

$$\frac{\mathrm{d}\kappa}{\mathrm{d}t} = \frac{\kappa^2 - 2\kappa + 1}{2\xi} - 2\xi\kappa, \kappa(0) = 0.$$

The solution to this equation is given by $\kappa(t) = 1 + 2\xi^2 - 2\xi\sqrt{1+\xi^2}\coth(\sqrt{1+\xi^2}t + 2\beta)$, where $\sinh(\beta) = \xi$. It can be verified that in case I, the optimal trajectory satisfies $(b/a)(t) = \kappa(t)$. After time τ, $(a-b)/2\xi$ becomes equal to 1 and the system switches to case II. Putting $(a-b)/2\xi = 1$ and $(b/a)(t) = \kappa(t)$, we get $r_2(\tau)/r_1(\tau) = 2\xi\kappa(\tau)/(1-\kappa(\tau))$ (denote this ratio by $\tan\theta_1$, see Fig. 5, Panel b). Then again by symmetry at time $T - \tau$ we have $1/2\xi(1/b - 1/a) = 1$ and the system switches from case II to case III. In case III, verify $(b/a)(t) = \kappa(T-t)$ and the switching to this case occurs at $\tan\theta_2 = r_2/r_1 = (1-\kappa(\tau))/2\xi$. Thus the system spends $T - 2\tau$ in region II. Then we have

$$T - 2\tau = \tan^{-1}\frac{1-\kappa(\tau)}{2\xi} - \tan^{-1}\frac{2\xi\kappa(\tau)}{1-\kappa(\tau)}.$$

Thus providing result (10).

We now derive an explicit expression for $r_2(T)$. For $t \geqslant T - \tau$,

$$V(t) = \sqrt{r_2^2(t) + \kappa(T-t)r_1^2(t)}, \quad \text{(B.4)}$$

is constant along the system trajectories and equals the optimal return function $r_2(T)$. At $t = T - \tau$, we have $r_2(T-\tau)/r_1(T-\tau) = \tan\theta_2 = (1-\kappa(\tau))/2\xi$ and therefore from (B.4), we have

$$V(T-\tau) = R_1\sqrt{\sin^2\theta_2 + \cos^2\theta_2 - 2\xi\sin\theta_2\cos\theta_2}, \quad \text{(B.5)}$$

where $R_1 = \sqrt{r_1^2(t) + r_2^2(t)}$ for $t = T - \tau$. Also note $V(T/2) = 2r_1(T/2)r_2(T/2)$. At time $t = T/2$, we then have $r_2/r_1 = \tan((\theta_1 + \theta_2)/2)$ and therefore

$$V\left(\frac{T}{2}\right) = R_2^2\sin(\theta_1 + \theta_2), \quad \text{(B.6)}$$

where $R_2 = \sqrt{r_1^2(T/2) + r_2^2(T/2)}$. Note between $T/2$ and $T - \tau$, the system evolves under $u_1 = u_2 = 1$. Therefore $R_1 = R_2\exp(-((T/2) - \tau))$. Since V is constant, equating (B.5) and (B.6), we get Eq. (11).

References

[1] R.R. Ernst, G. Bodenhausen, A. Wokaun, Principles of Nuclear Magnetic Resonance in One and Two Dimensions, Clarendon Press, Oxford, 1987.
[2] S.J. Glaser, T. Schulte-Herbrüggen, M. Sieveking, O. Schedletzky, N.C. Nielsen, O.W. Sørensen, C. Griesinger, Unitary control in quantum ensembles, maximizing signal intensity in coherent spectroscopy, Science 208 (1998) 421–424.
[3] A.G. Redfield, The theory of relaxation processes, Adv. Magn. Reson. 1 (1965) 1–32.
[4] M. Goldman, Interference effects in the relaxation of a pair of unlike spin-1/2 nuclei, J. Magn. Reson. 60 (1984) 437–452.
[5] G.A. Morris, R. Freeman, Enhancement of nuclear magnetic resonance signals by polarization transfer, J. Am. Chem. Soc. 101 (1979) 760–762.
[6] D.P. Burum, R.R. Ernst, Net polarization transfer via a *J*-ordered state for signal enhancement of low-sensitivity nuclei, J. Magn. Reson. 39 (1980) 163–168.
[7] R. Bellman, Dynamic Programming, Princeton University Press, Princeton, 1957.